# Efficient direct calculation of complex resonance (Siegert) energies

Hyo Weon Jang and John C. Light
*Department of Chemistry and The James Franck Institute, The University of Chicago, Chicago, Illinois 60637*
(Received 28 June 1994)

An improved version of the Siegert method to calculate resonance state parameters directly is presented. A prediagonalization of the Hamiltonian in a real $L^2$ basis and an equation partitioning technique are utilized along with an inverse iteration method (combined with a rational fraction root search) to find accurate positions and widths of narrow resonances. Model calculations suggest that the present method is efficient and accurate especially for narrow resonances regardless of the potential range.

PACS number(s): 34.10.+x

## I. INTRODUCTION

One can divide the various exact theoretical methods of resonance structure calculations according to whether the resonance parameters (position $E_r$ and width $\Gamma$) are determined directly or indirectly. The so called Siegert method [1–5], along with the complex scaling approach [6], and the optical potential method [7], finds them directly as a complex resonance energy. Other methods, such as stabilization [8], time delay maximum analysis [9,10], eigenphase analysis [11], and the $S$-matrix parametrization [12] may be exact but require extraction of the resonance parameters from the background contributions. The direct methods may be more convenient to apply, especially when the background effects are not negligible or depend strongly on the scattering energy (e.g., just above the threshold with many bound states).

The Siegert methods proposed thus far have several common characteristics. They determine the resonance energies as the resonance poles of the $S$ matrix (i.e., the complex Siegert energies whose corresponding states are purely outgoing and diverging asymptotically) on the second sheet of complex energy plane, each located at an $E_S = E_r - i\Gamma/2$ ($E_S$ denotes the Siegert energy and $E_r$, $\Gamma$ are the position and width of the resonance state, respectively). Since a resonance energy $E_S$ occurs nonlinearly in the equation that must be solved to determine the poles, and $E_S$ is not known initially, some kind of iteration scheme is inevitably needed to solve the equations. Finally, as a result of the matrix variational procedures used to solve for all the poles of the $S$ matrix, one obtains not only the resonance poles but also the direct scattering poles, also called "false" or "cutoff" poles. Thus, there is a need to distinguish between the two kinds of poles [5], the resonance poles of interest having relatively narrow widths in favorable cases.

Depending on where one applies the asymptotic boundary condition for the Siegert wave functions, one can use either an infinite or a finite range of the scattering coordinate. In the infinite range versions, one must be careful in evaluating the matrix element integrals to avoid divergences caused by diverging Siegert wave functions. Analytic continuation [3] and combined evaluation of the $\hat{H} - E$ operator [4] have been successfully used in this regard. Also, some of the basis functions must behave like the Siegert wave functions asymptotically in order to satisfy the required boundary conditions. On the other hand, in the finite range versions [1,5], the basis functions may be fixed functions which simplifies the matrix element evaluation requirements. The information determining the Siegert energies is introduced into the equations through the Bloch operator [13], which fixes the boundary conditions at finite range. This finite range version is suitable for short-range potentials, but even with long-range potentials this may be still useful, as exemplified later in our model calculations. One can also include the long-range part of the potential in the asymptotic boundary conditions, leaving only the remaining short-range part to be taken care of by the basis set [4].

The problem of scattering poles versus resonance poles is shared by the complex scaling method, although the expected locations of the scattering poles are simpler to determine in the complex scaling method [6]. Because no poles are found below the string of scattering poles in the complex energy plane, one may not expect to find resonance poles near or below the string accurately or at all. The location of the string of scattering poles in the complex energy plane is a function of the potential and the basis set range in the Siegert method, and of the coordinate rotation angle $\theta$ in the complex scaling method. Since $\theta$ can be chosen to be any value between 0 and $\pi/2$, there is no concern about missing resonance poles in the complex scaling method, in principle. But, in the Siegert method, there is less control over the position of the scattering poles. Thus, some of the broad resonance poles may be "hidden" or "displaced," and one must resort to some kind of correction scheme in some cases to find them [5]. This will be tested in the model calculations below. However, if one is interested in the broad resonances especially, it might be useful to use other methods rather than the Siegert method, such as the time delay maximum analysis [9,10], the complex scaling [6], or the optical potential methods [7].

 

In the complex scaling and the optical potential methods, many diagonalizations of large (size of the basis set) matrices are required before one finds the stable (highly accurate) values of the resonance poles. In the Siegert method, however, the iteration may not necessarily involve many large matrix diagonalizations, which is relevant to the focus of this paper.

In this paper, our purpose is to improve the computational efficiency in determining directly the resonance parameters using a finite range basis and focusing primarily on the iteration stage. A prediagonalization of a real Hamiltonian matrix using a finite range basis is done to obtain good initial guesses of the resonance pole locations. We then use a new iteration procedure to facilitate the calculations. In the equation partitioning technique, the matrix size of the iterative eigenproblem reduces to $(N_{open}+1)\times(N_{open}+1)$ ($N_{open}$ denotes the number of open channels), and the accompanying large matrix inversion is replaced by a simple summation. This small complex eigenproblem is solved by the standard inverse iteration method [14] with some necessary modification until a converged eigenvalue is obtained. *The overall procedure completely avoids any iterative diagonalization or iterative inversion of the full matrix.*

Using the basis set $R$-matrix theory [15], one can also extract the resonance parameters following a single full real matrix diagonalization. The $S$ matrix at any energy is easily determined by analyzing the eigenvalues and eigenvectors of the Hamiltonian matrix represented by basis functions satisfying the $R$-matrix boundary conditions. The subsequent analysis of the energy dependence of the $S$ matrix produces the resonance parameters. Also, the variational $R$-matrix method can be used to avoid the slow convergence problem in the original theory.

Also, Bowman and co-workers diagonalized a single full real Hamiltonian matrix to obtain a good truncated basis set in which to represent a complex Hamiltonian modified with an optical potential. They then used this smaller complex matrix to study resonances and photodissociation [16,17].

The inverse iteration method was used with a full complex matrix to determine a small number of (resonance) eigenvalues and eigenvectors when good initial guesses were available from the previous calculations in the complex scaling method [18]. In these cases, the Lanczos recursion method [19] could also be used for the same purpose. Both methods are more efficient than the full matrix diagonalization.

Additional efficiency with negligible (or little) loss of accuracy is obtained by adopting continuum-type functions which depend only on the initial guess of the real part of the resonance energy. Thus, the frequency of energy dependent matrix element integral reevaluations is greatly reduced. Finally, with a limited size basis set, it is shown to be useful to increase the definition range of the Siegert wave function (or, equivalently, the integration range of the continuum-type basis functions) beyond that of the bound-type basis functions. This recovers the residual effects of the potential beyond the bound-type basis function range. This improves the results with little extra effort. In Sec. II we present the theory and algorithm used; in Sec. III we present several model calculations of shape and Feshbach resonances with the comparisons of approaches; and in Sec. IV we briefly present our conclusions.

## II. METHOD

### A. Basis and equation partitioning

We restrict our notation to a one-dimensional $s$-wave scattering case for simplicity, and generalize later. The basic approach of the Siegert method is to solve the Schrödinger equation (in atomic units) of the system of mass $m$ with outgoing boundary conditions at $r=P$ (i.e., $\hat{L}\Psi_S=0$) for the complex eigenenergy $E_S$. This equation can be written as [13]

$$\left(\hat{H}+\hat{L}-E_S\right)\Psi_S=0, \tag{1}$$

where the Bloch operator $\hat{L}$ is

$$\hat{L}=\hat{L}(E_S)=\frac{1}{2m}\delta(r-P)\left(\frac{d}{dr}-ik_S\right).$$

The Hamiltonian operator $\hat{H}$ is defined as that of the usual radial motion with the volume element $d\tau = dr\sin\theta d\theta d\phi$. If the complex wave number $k_S$ (with negative imaginary part) is given by the eigenenergy $E_S=\frac{k_S^2}{2m}$, then the solution $E_S$ is the Siegert energy and $\Psi_S$ is the Siegert wave function if they are independent of $P$.

To save computation during the iterative solving of these equations, we diagonalize the Hamiltonian matrix in a real subset of translational basis functions which is composed of bound-type functions only (satisfying zero boundary conditions at both ends of the basis set range). This prediagonalization of one real large matrix yields two major rewards in the later iteration stage. First, in the search for resonance poles, we have to deal with only small size (number of open channels plus one) matrix eigenproblems not involving any large matrix inversion or diagonalization, instead of the usual large matrix eigenproblems. Second, the discrete eigenvalues serve as good initial guesses of the resonance energies which is the basic idea behind the stabilization method [8].

Unlike the infinite range version, the finite range version allows us to use fixed energy independent continuum-type basis functions in place of the usual Siegert energy dependent functions. In this case, the matrix elements are less frequently reevaluated than otherwise without much loss of accuracy in the final result (hopefully).

Regarding the iteration scheme, we find that the individual eigenvalue hunting inverse iteration method [14] is efficient and avoids some wasteful computation if we ever use the iterative diagonalization method, since only one eigenvalue is the consistent and meaningful Siegert energy only when we solve for a matrix with the Siegert

energy. In the inverse iteration process, we may use the refined eigenvalue to define the matrix of the eigenproblem for the next iteration. In this way, the eigenvalue and the eigenproblem are refined and converge at the same time. We can boost the convergence speed by adding a root search tool virtually at any point along the above iteration thread as needed.

Thus, to start we diagonalize $\hat{H}$ in a real sub-basis set on a range of $[O,P]$. Then, to proceed with the above, we expand $\Psi_S$ in a finite basis set defined on the same range $[O,P]$ as

$$\Psi_S = c_0\phi_0 + \sum_{i=1}^{N-1} c_i\phi_i, \tag{2}$$

where $\phi_i$ $(i \geq 1)$ are the orthonormalized bound-type discrete eigenfunctions of $\hat{H}$ in the above mentioned sub-basis set and $\phi_0$ is a continuum-type function with the boundary condition imposed to satisfy $\phi_0(O) = 0$, $\phi_0(P) \neq 0$. The definition range $[O,P]$ must be chosen such that $O$ is located at the origin or in the classically forbidden region where $\Psi_S(O) \approx 0$ and $P$ is in the asymptotic region. The bound-type basis functions may be defined on a smaller region for a particular choice of $\phi_0$ (see below for detail), such as $[O,Q]$, $Q < P$. In this case, the $\phi_i$ $(i \geq 1)$ vanish in $[Q,P]$.

By applying the usual variational procedure to Eqs. (1) and (2), one obtains a matrix secular equation that can be cast as a matrix eigenproblem,

$$(\mathbf{H} - E_S\mathbf{D})\,\mathbf{c} = \mathbf{0}, \tag{3}$$

where

$$\mathbf{H}_{ij} = \mathbf{H}_{ij}(E_S) = \int_O^P dr\phi_i(r)\left(\hat{H} + \hat{L}\right)\phi_j(r),$$

$$\mathbf{D}_{ij} = \int_O^P dr\phi_i(r)\phi_j(r).$$

Only the matrix elements involving $\phi_0$ may depend on $E_S$ (depending on how we choose $\phi_0$), while the others are constant. Thus, the submatrix of $\mathbf{H}$ not involving $\phi_0$ is a diagonal matrix of discrete eigenvalues and the similar submatrix of $\mathbf{D}$ is a unit matrix. Note that the full $\mathbf{H}$ is complex symmetric since $\hat{L}$ is not a Hermitian operator; therefore, a biorthogonal basis set must be used [13].

We wish to solve Eq. (3) for many values of $E_S$ including all resonances. To solve it efficiently by iteration for values of $E_S$, for example, from the $m$th discrete eigenvalue $\epsilon_m$, we partition $\mathbf{H}$ and $\mathbf{D}$ into "$a$" and "$b$" blocks as

$$\mathbf{H} = \begin{bmatrix} \mathbf{H}_{aa} & \mathbf{H}_{ab} \\ \mathbf{H}_{ba} & \mathbf{H}_{bb} \end{bmatrix},$$

$$\mathbf{D} = \begin{bmatrix} \mathbf{D}_{aa} & \mathbf{D}_{ab} \\ \mathbf{D}_{ba} & \mathbf{D}_{bb} \end{bmatrix},$$

where $a$ involves the continuum-type function and the $m$th bound-type discrete eigenfunction, and $b$ involves the remaining $N-2$ bound-type discrete eigenfunctions.

We can now rearrange the full eigenproblem into two smaller coupled problems. With standard matrix partitioning, the $a$ eigenproblem alone can be written exactly as

$$(\mathbf{M} - E_S\mathbf{D}_{aa})\,\mathbf{c}' = \mathbf{0}, \tag{4}$$

where

$$\mathbf{M} = \mathbf{M}(E_S) = \mathbf{H}_{aa} - (\mathbf{H}_{ab} - E_S\mathbf{D}_{ab}) \times (\mathbf{H}_{bb} - E_S)^{-1}(\mathbf{H}_{ba} - E_S\mathbf{D}_{ba}) \tag{5}$$

and

$$\mathbf{c}' = (c_0, c_m)^T.$$

Note that $(\mathbf{H}_{bb} - E_S)^{-1}$ is a diagonal matrix composed of the inverse of the discrete eigenvalues minus $E_S$ and that we used the fact that $\mathbf{D}_{bb}$ is a unit matrix. Thus, the second term of Eq. (5) is easily evaluated by summation. As a result, we only have to solve this $2\times 2$ eigenproblem of Eq. (4) iteratively until converged. We may view $\mathbf{M}$ of Eq. (5) as $\mathbf{H}_{aa}$ giving the direct coupling between the continuum-type state and the $m$th bound-type state, which is the minimal requirement to describe a resonance. The second term represents the remaining coupling via the other bound-type functions. For a multichannel case, the size of small eigenproblem becomes the number of open channels plus one. After solving the multichannel problem, the eigenvector $\mathbf{c}'$ can be used to determine the partial widths.

There is no *a priori* requirement for choosing the $(2, N-2)$ partition; however, we found that this is highly advantageous with respect to efficiency and stability in the iteration procedure compared to other partitions. Indeed, the $(1, N-1)$ partition was suggested by Yaris, Lovett, and Winkler [4] as a form of determinant equation instead of an eigenproblem and was also implied in the $S$-matrix expression involving log derivative matrix given by Manolopoulos, D'Mello, and Wyatt [20].

As pointed out earlier, because $E_S$ already enters through the Bloch operator in the equations, we can choose any proper basis functions and are not required to include explicitly a Siegert-type continuum function. We tried three different continuum-type functions; they are (1) a totally energy dependent (ED) Siegert-type function, $g(r)e^{ik_S r}$; (2) a partially energy dependent (PED) function, $g(r)e^{ik_m r}$; and (3) a totally energy independent (EI) function, $g(r)$, where $g(r)$ is a usual cutoff function (or an auxiliary function) satisfying $g(r \to O) = 0, g(r \to P) = 1$. [In the model calculations below we used $S$-shape $g(r)$ functions.] The complex wave number $k_S$ is determined by $E_S$, while the real $k_m$ is determined by each "special" discrete eigenvalue $\epsilon_m$ (the one included in the initial $a$ partition). The ED case has been used previously by many workers [2–4], which is natural if we want to represent $\Psi_S$ by the $\phi_i$'s $(i \geq 1)$ in the interaction region and solely by the $\phi_0$ in the asymptotic region. (In the infinite range version of the Siegert method, this is the only proper choice among the above three.) The EI case was implicitly suggested by Manolopoulos, D'Mello, and Wyatt in their $S$-matrix calculation method involv-

ing energy independent integrals [20]. The major role of $\phi_0$, in this case, is to prevent the wave function from vanishing at the outer end ($P$) of the definition range. In the EI case, the $\phi_i$'s ($i \geq 1$) must represent the wave function (with $\phi_0$) throughout the interaction and asymptotic region, which suggests that the bound-type basis functions must "work harder" in the EI case than in the ED case. On the other hand, the PED case is examined for the first time in this work, to the best of our knowledge. Our motivation is that since for a narrow resonance, $k_S \approx k_m$, we may expect about the same efficiency from $g(r)e^{ik_m r}$ as for $g(r)e^{ik_S r}$ in representing the Siegert wave function in the asymptotic region *but with much saving in the matrix element integral evaluations.* This advantage is borne out by the model calculations.

The three choices of $\phi_0$ entail differences regarding the accuracy of the calculated $E_S$, the frequency of integral evaluations during the iteration, the required basis set density, and the compatibility with the use of truncated discrete eigenfunctions as bound-type basis functions (e.g., those of a successive diagonalization-truncation scheme [21]). These aspects will be tested in the model calculations below.

### B. Iterative solution

To find the possible resonance poles without any prior knowledge of their locations, we start with the real discrete eigenvalues $\epsilon_m$ and use each of them sequentially instead of $E_S$ in $\mathbf{M}(E_S)$ of Eq. (5). This defines the first eigenproblem in each $\epsilon_m$ iteration thread. Thus, the initial guess of eigenvalue (i.e., $E_S$) is chosen as $\epsilon_m$ and eigenvector as $(0,1)^T$ or $(1,1)^T$. The refined eigenvalue and eigenvector are given by the individual eigenvalue hunting inverse iteration method [14] as

$$\mathbf{c}'^{(n+1)} = (\mathbf{M} - E^{(n)})^{-1}\mathbf{D}_{aa}\mathbf{c}'^{(n)},$$

$$E^{(n+1)} = E^{(n)} + \frac{\mathbf{c}'^{(n)^T}\mathbf{D}_{aa}\mathbf{c}'^{(n)}}{\mathbf{c}'^{(n+1)^T}\mathbf{D}_{aa}\mathbf{c}'^{(n)}},$$

where $(n)$ and $(n+1)$ denote $(n)$th and $(n+1)$th inversion results, respectively. In our actual calculations, $\mathbf{c}'^{(n+1)}$ is determined as the solution of a system of linear equations using the standard LU decomposition [14], not explicitly involving matrix inversion. The refined eigenvector $\mathbf{c}'^{(n+1)}$ is normalized before it is used for the next iteration step. We can use $E^{(n+1)}$ to refine the $\mathbf{M}$ at each inversion or postpone this until a converged eigenvalue is obtained for a given $\mathbf{M}(E^{(n)})$. The latter choice requires more iterations with no noticeable difference in the final converged results of $E_S$ in the model calculations. However, it produces smoother trajectories of $E^{(n)}$'s toward the final values [in this case, $E^{(n+1)}$ denotes the somewhat converged eigenvalue for a particular $\mathbf{M}(E^{(n)})$].

Another tool which helps to speed up the convergence along the iteration thread is to construct a rational fraction $T$ determined by several $(E^{(n)}, E^{(n+1)})$ data pairs as [14,22]

$$T(E^{(n)}) - E^{(n+1)} = 0$$

and subsequently to find the root $E$ of the equation $T(E) - E = 0$ numerically to predict the approximate location of $E_S$. This root is used as the input value for constructing $\mathbf{M}$ for the next iteration step. This convergence boosting step can be inserted at any point along the iteration thread as needed (probably except at the early stage since there are not enough data pairs to use). It is found that this procedure helps to improve the convergence speed substantially, especially for the poles with large magnitude imaginary values.

The combination of the above two methods starting from a particular $\epsilon_m$ is applied repeatedly until one finds a converged eigenvalue (either resonance or scattering pole). In practice, not every iteration thread leads to a converged value within a given maximum number of iterations; however, almost all of the failed threads have large magnitude imaginary values at the last iteration step, which means that they are probably converging to the scattering poles of no interest. If one is interested only in "real" resonances with lifetimes exceeding a chosen limit, then one can truncate all pole searches at a chosen maximum $\Gamma$. The pole search iteration trajectory appears sufficiently monotonic to permit this procedure (see Sec. III).

The major computation requirements incurred by the above algorithm to find many resonance and scattering poles are (1) a single large real Hamiltonian matrix diagonalization; (2) two large rectangular matrix evaluations involving the continuum-type functions (part of $\mathbf{H}$ and $\mathbf{D}$)—this is required only once for all iteration threads in the EI case, once for each thread in the PED case, or every time the $\mathbf{M}$ matrix is revised in the ED case; (3) small matrix inversion (or a solution of a system of linear equations) at every step of the iteration; and (4) rational fraction constructions and root finding as needed.

Even though it may not be a major difficulty in practice (one is normally interested in narrow resonances), we need a means to distinguish resonance poles from the scattering poles, in principle. One way is to use the fact that the locations of resonance poles are not affected by changing the calculation parameters such as the definition range of the bound-type functions or of the Siegert wave function. The other way is to use the prediction formula of scattering poles which states that $\mathrm{Im}\{k_S\} \approx (2P)^{-1}\ln[(2\mathrm{Re}\{k_S\})^{-2}|\mathrm{V}(P)|]$ when $\mathrm{Re}\{Pk_S\}$ is sufficiently large, or $\mathrm{Im}\{k_S\} \approx -\frac{\alpha}{2}$ if the potential behaves like $e^{-\alpha r}$ asymptotically [5].

As mentioned earlier, the Siegert method has an inherent difficulty in producing accurate values for broad resonances (to be precise, the poles near or below the scattering pole string). In this case, one may want to use a correction scheme such as the perturbative correction proposed by Meyer and Walter [5]. We will try a simple WKB-type boundary condition correction in the model calculations [i.e., replacing $E_S$ by $E_S - \mathrm{V}(P)$]. However, when it gets cumbersome to apply a correction scheme, it may be better to use other recognized methods, such as time delay maximum analysis [9,10], complex scaling [6], or an optical potential method [7], which are free of this restriction in principle. As mentioned above, however, narrow resonances corresponding to poles near the real axis are much more easily found by the present method.

## III. MODEL CALCULATIONS

The first example is the one-dimensional radial problem [10] with a long-range potential of the Lennard-Jones form, $V_0[(\frac{\alpha}{x})^{12} - 2(\frac{\alpha}{x})^6]$. The basis set representation of the Hamiltonian operator is done by the discrete variable representation (DVR) based on Lobatto shape functions [23]. The integrations are done with the same DVR quadratures. The outgoing Riccati-Hankel function is used to define the Bloch operator. Plane waves are used for the ED continuum-type functions. The parameters are chosen to represent a weakly bound van der Waals molecule. They are mass $m = 1.92$ g/mol, $\alpha = 3.56$ Å, and the angular momentum $J = 8$.

We calculated typical narrow ($V_0 = 60$ cm$^{-1}$) and broad shape resonance ($V_0 = 40$ cm$^{-1}$) poles to check how the finite cutoff radius affects the results. As one can see from Table I and Fig. 1, the narrow resonance allows very accurate values while the broad one does not because of the proximity of the scattering pole string. In Table I, we compare the values obtained with a simple WKB-type boundary condition with those using the exact asymptotic boundary condition. It is seen that the simple change in the boundary condition helps to obtain more stable values especially for the broad resonance. Even with this finite cutoff radius for a long-range potential, we still can obtain very accurate values at least for narrow resonances. The detailed iteration trajectories are given in Fig. 2. We can see their pseudolinearity, which immediately suggests a useful criterion for picking out poles with a predetermined maximum width, i.e., we can stop the iteration (therefore, avoid wasteful calculations) once we pass a given value of $\Gamma$ in the iteration corresponding to a given minimum lifetime of interest. Note that some results of Table I are plotted in Figs. 1 and 2.

The second example is the two-dimensional Secrest-Johnson collinear vibrational excitation problem with a coupling Morse potential. The Hamiltonian operator is given by

$$\hat{H} = -\frac{1}{m}\frac{\partial^2}{\partial x^2} + \left(\frac{\partial^2}{\partial y^2} + y^2\right) + V_0\left(e^{-\alpha(x-y)} - 2e^{-\frac{\alpha}{2}(x-y)}\right).$$

The basis set representation of $\hat{H}$ is done by a DVR based on one-dimensional box eigenfunctions (sine functions vanishing at both ends) for $x$ and harmonic oscillator eigenfunctions for $y$. The continuum-continuum matrix element evaluations are done with accurate quadratures (Gauss-Lobatto). Also, for the continuum-bound matrix element evaluations, the same accurate quadratures are used for EI, while the DVR quadratures are used for ED and PED since they were found to be sufficiently accurate with much simpler summations. The appropriateness of the DVR quadratures for continuum-bound integral evaluations for ED and PED may be understood, at least partly; since the integrands of these integrals of the combined operator $\hat{H} + \hat{L} - E_S$ vanish (or approximately vanish for PED) asymptotically as the interaction potential vanishes, they may be accurately evaluated by quadratures based on one-dimensional box eigenfunctions. In the EI case, however, the corresponding integrands do not vanish asymptotically, thus the integrals may be poorly evaluated by the above quadratures.

The parameters chosen here are the ones used before [10,24], i.e., $m = 0.2$, $V_0 = 1.5$, $\alpha = 0.1$. (This potential has Feshbach resonances for vibrational states $n_y = 1, 2, 3, \ldots$ .) For this example, we used only the exact asymptotic boundary conditions. We applied the present real diagonalization followed by complex inverse iteration method and found many converged poles (in principle, the same as the number of starting discrete

TABLE I. The effect of cutoff radius and use of two different boundary conditions. Basis is 80 bound-type Lobatto shape functions plus one ED continuum-type function.

| | $V_0 = 60$ cm$^{-1}$ | | $V_0 = 40$ cm$^{-1}$ | |
|---|---|---|---|---|
| Range (Å)[a] | Asymptotic[b] | WKB type[c] | Asymptotic | WKB type |
| [2, 20] | 9.493 31[d] | 9.493 35 | 17.63 | 17.64 |
| | 0.132 16[e] | 0.132 16 | 3.30 | 3.27 |
| [2, 40] | 9.493 35 | 9.493 35 | 17.53 | 17.64 |
| | 0.132 17 | 0.132 17 | 3.26 | 3.26 |
| [2, 45] | 9.493 35 | 9.493 35 | 17.90[f] | 17.64 |
| | 0.132 17 | 0.132 17 | 3.37[f] | 3.27 |

[a] $[O, Q]$ (bound-type function range) = $[O, P]$ (integration range), see text for details.
[b] Exact asymptotic energy $E_S$ is used for the Bloch operator evaluation and for the ED continuum-type function definition.
[c] Local asymptotic energy $E_S - V(P)$ is used for the Bloch operator evaluation and for the ED continuum-type function definition.
[d] $E_r$ in cm$^{-1}$, the real part of complex resonance energy, the same for other entries.
[e] $\Gamma/2$ in cm$^{-1}$, negative of the imaginary part of complex resonance energy, the same for other entries.
[f] The pole with the smallest magnitude imaginary wave number, see Fig. 1(b).

eigenvalues) in the real energy interval of 1–7 (the thresholds are at 1, 3, 5, 7, ...). They are displayed in Fig. 3 for a particular calculation. Note that the resonance poles are clearly distinguished from the scattering poles for this narrow resonance problem and that the resonance poles are independent of the integration range. The effects of using each of three different continuum-type functions and use of successive diagonalization-truncation (SDT) bound-type basis functions on the resonance pole values are examined in Table II along with the total CPU times on a Stardent GS2000 computer required to find many (more than 100) poles. It is seen that PED is the best regarding the CPU time and accuracy while EI is capable of producing only rough values for the same bound-type basis set. We confirmed that EI gives the same results as ED or PED when a sufficiently dense basis set is used. The SDT basis set results in the right two columns compare better to the accurate results of the left two columns

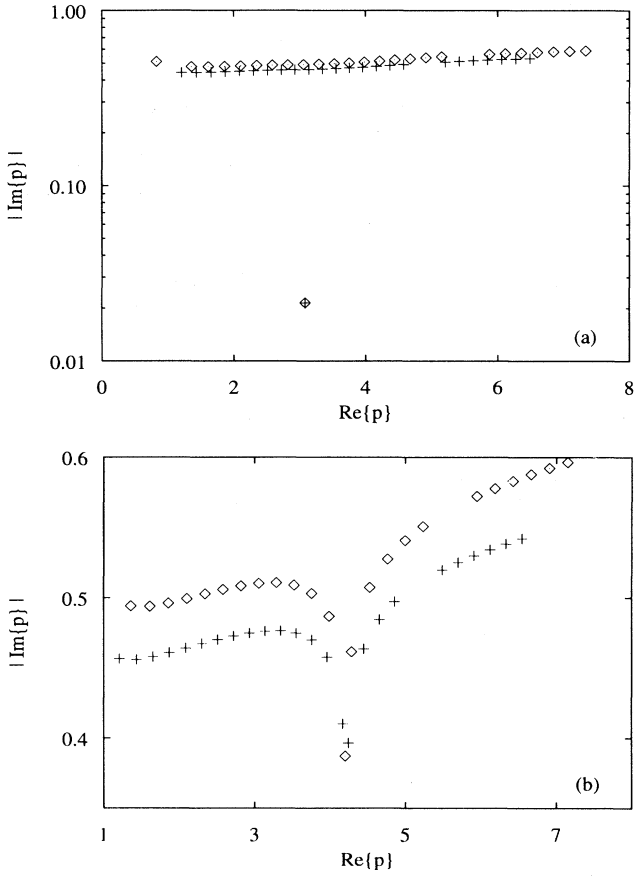


FIG. 1. Effect of cutoff radius on narrow and broad resonances. We show the positions of the poles in the square root complex energy plane (p denotes $\left[E(\text{ cm}^{-1})\right]^{\frac{1}{2}}$). The basis is same as that of Table I, and the integration range is [2 Å, $P$]. $P = 40$ Å results are denoted by ($\diamond$), and $P = 45$ Å results by (+). The ED case is used using the exact asymptotic boundary conditions. (a) A narrow resonance ($V_0 = 60$ cm$^{-1}$) allows accurate values; (b) a broad resonance ($V_0 = 40$ cm$^{-1}$) needs the WKB-type boundary condition to obtain a better result (see Table I.). Note that the scales are different.

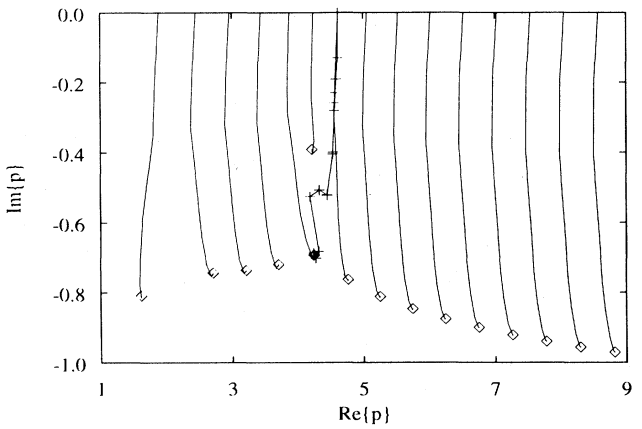


FIG. 2. Pseudolinearity of the iteration trajectory on the square root complex energy plane (p denotes $\left[E(\text{ cm}^{-1})\right]^{\frac{1}{2}}$). The basis is the same as that of Table I, and the integration range is [2 Å, 20 Å], $V_0 = 40$ cm$^{-1}$. The ED case is used using the exact asymptotic boundary conditions. The smoothness of the trajectory depends on the iteration parameters such as the number of data pairs used for rational fraction construction, the frequency of revision of the eigenproblem. Different parameters may give rough trajectory as exemplified by the crossed (+) one. For example, the smooth trajectory leading to the common pole involves 30 inverse iterations and 8 root search while the rough one involves 15 and 10, respectively.

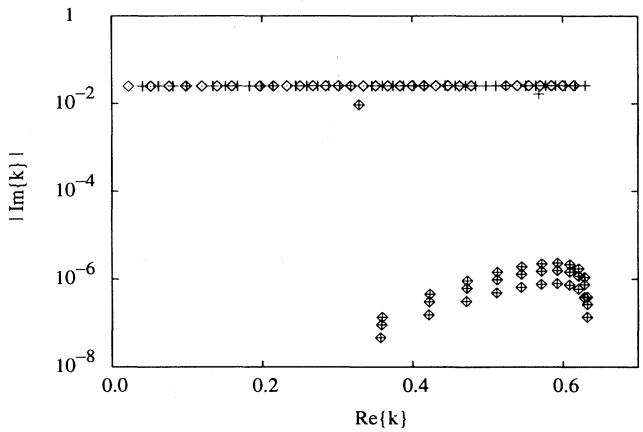


FIG. 3. Distributions of scattering and resonance poles and the effect of using two different integration ranges displayed on the complex wave number (of the highest asymptotic vibrational state channel) plane. The parameters are 7/80, [−30, 200] (= $[O, Q]$) and the ED case is used. The integration range is $[-30, P]$. Thirty-three resonance and 96 scattering poles of the $P = 200$ case are denoted by ($\diamond$), and 33 resonance and 103 scattering poles of the $P = 230$ case by (+). The three scattering poles deviating from the straight line with $|\text{Im}\{k\}| \approx 0.25$ ($\approx \frac{\alpha}{4}$, see Sec. II for details) are caused by insufficient basis set density and/or range. Note that many scattering poles appear to be superimposed and, also, that only one diagonalization is involved for these two ranges.

TABLE II. The effect of using three different continuum-type functions and SDT bound-type basis functions.

| | 7/80,[a][-30,200],[-30,200][b] | | 7/60(80),[c][-30,200],[-30,200] | |
|---|---|---|---|---|
| $(n_x, n_y)$[d] | PED(ED)[e] | EI | PED(ED)[e] | EI |
| (0,1) | 1.639 010 207[f] | 1.639 010 208 | 1.639 010 207 | 1.639 010 210 |
| | 1.67[-7][g] | 1.67[-7] | 1.67[-7] | 1.68[-7] |
| (1,1) | 1.887 026 277 | 1.887 026 283 | 1.887 026 277 | 1.887 026 293 |
| | 6.52[-7] | 6.57[-7] | 6.52[-7] | 6.66[-7] |
| (3,1) | 2.308 357 655 | 2.308 357 633 | 2.308 357 656 | 2.308 357 593 |
| | 2.52[-6] | 2.58[-6] | 2.52[-6] | 2.67[-6] |
| (9,1) | 2.973 988 565 | 2.973 988 457 | 2.973 988 585 | 2.973 988 290 |
| | 2.41[-6] | 2.36[-6] | 2.44[-6] | 2.27[-6] |
| (0,2) | 3.642 629 839 | 3.642 629 841 | 3.642 629 839 | 3.642 629 845 |
| | 3.30[-7] | 3.31[-7] | 3.30[-7] | 3.32[-7] |
| (1,2) | 3.890 344 247 | 3.890 344 261 | 3.890 344 246 | 3.890 344 283 |
| | 1.29[-6] | 1.30[-6] | 1.29[-6] | 1.31[-6] |
| (9,2) | 4.974 528 420 | 4.974 528 224 | 4.974 528 454 | 4.974 527 870 |
| | 4.73[-6] | 4.61[-6] | 4.89[-6] | 4.51[-6] |
| (0,3) | 5.646 223 149 | 5.646 223 153 | 5.646 223 149 | 5.646 223 158 |
| | 4.91[-7] | 4.92[-7] | 4.91[-7] | 4.92[-7] |
| (1,3) | 5.893 637 055 | 5.893 637 079 | 5.893 637 054 | 5.893 637 113 |
| | 1.92[-6] | 1.93[-6] | 1.92[-6] | 1.95[-6] |
| CPU times (sec) | 423[h](1488[i]) | 426 | 250(935[i]) | 262 |

[a]Bound-type basis set, [$y$ functions]/[$x$ functions].
[b]$[O, Q]$ (bound-type function range), $[O, P]$ (integration range).
[c]SDT basis set, 80 $x$ functions contracted to 60, then recoupled with 7 $y$ functions.
[d]Zeroth order vibrational quantum number of resonance state.
[e]All significant figures identical for ED and PED (however, not for the scattering pole values not listed here).
[f]$E_r$, the real part of complex resonance energy, the same for other entries.
[g]$\Gamma/2$, negative of the imaginary part of complex resonance energy (the number in brackets is the power of 10), the same for other entries.
[h]Partitioned to 186 sec for constructing and diagonalizing a real Hamiltonian matrix and 237 sec for finding 179 poles (including all 33 resonance poles) starting from 187 discrete eigenvalues. The remaining 8 failed to be converged.
[i]CPU times for ED.

for ED and PED than do the EI results. These comparisons indicate that the basis set requirements for the EI case are more stringent than for the ED and PED cases.

As mentioned in the preceding section, it is not necessary that the integration range of the matrix elements (or the Siegert wave function definition range) $[O, P]$ be the same as the range of the bound-type basis functions $[O, Q]$. We can increase the integration range outward arbitrarily since the continuum-type function already behaves like the Siegert wave function in the extended region $[Q, P]$ in the ED and PED (approximately) cases if we use a proper cutoff function. In this way, we can recover, at least partly, any residual effect of the potential beyond the bound-type basis function range. A test of this with much restricted calculations is shown in Table III. The bound-type basis was restricted to a small range, while the integration range was also restricted or expanded, as in Table III. The larger integration range results of the right column compare considerably better to the extensive calculations of Table II than do the fully restricted range calculations of the left column. Note the great reduction in CPU times (a factor of 7 $\sim$ 11 with

TABLE III. Correction by increasing the integration range. See Table II for notes.

| | 7/30,[-30,60],[-30,60] | 7/30,[-30,60],[-30,200] |
|---|---|---|
| $(n_x, n_y)$ | PED(ED)[a] | PED(ED)[a] |
| (0,1) | 1.639 010 224 | 1.639 010 206 |
| | 1.70[-7] | 1.66[-7] |
| (1,1) | 1.887 026 306 | 1.887 026 273 |
| | 6.13[-7] | 6.54[-7] |
| (3,1) | 2.308 357 789 | 2.308 357 649 |
| | 2.54[-6] | 2.51[-6] |
| (0,2) | 3.642 629 873 | 3.642 629 836 |
| | 3.36[-7] | 3.29[-7] |
| (1,2) | 3.890 344 306 | 3.890 344 239 |
| | 1.22[-6] | 1.30[-6] |
| (0,3) | 5.646 223 199 | 5.646 223 145 |
| | 5.01[-7] | 4.89[-7] |
| (1,3) | 5.893 637 147 | 5.893 637 044 |
| | 1.81[-6] | 1.93[-6] |
| CPU times (sec) | 59(128[b]) | 55(133[b]) |

[a]All significant figures identical for ED and PED.
[b]CPU times for ED.

TABLE IV. Comparison of resonance positions and widths from the present method, the time delay maximum analysis and the complex scaling method. See Table II for notes.

| $(n_x, n_y)$ | Present[a] | Time delay maximum analysis[b] | Complex scaling[c] |
|---|---|---|---|
| (0,1) | 1.639 010 207 | 1.639 101 207 | 1.639 010 208 |
| | 1.67[-7] | 1.67[-7] | 1.66[-7] |
| (1,1) | 1.887 026 277 | 1.887 026 277 | 1.887 026 278 |
| | 6.52[-7] | 6.51[-7] | 6.52[-7] |
| (3,1) | 2.308 357 655 | 2.308 357 655 | (2.308 315 185) |
| | 2.52[-6] | 2.52[-6] | (-3.60[-5]) |
| (9,1) | 2.973 988 565 | 2.973 988 564 | — |
| | 2.41[-6] | 2.41[-6] | — |
| (0,2) | 3.642 629 839 | 3.642 629 839 | 3.642 629 841 |
| | 3.30[-7] | 3.31[-7] | 3.31[-7] |
| | 3.30[-7],2.03[-10][d] | — | — |
| (1,2) | 3.890 344 247 | 3.890 344 246 | 3.890 344 249 |
| | 1.29[-6] | 1.29[-6] | 1.30[-6] |
| | 1.29[-6],1.10[-9] | — | — |
| (9,2) | 4.974 528 420 | 4.974 528 421 | — |
| | 4.73[-6] | 4.73[-6] | — |
| | 4.73[-6],4.92[-9] | — | — |
| (0,3) | 5.646 223 149 | 5.646 223 149 | 5.646 223 153 |
| | 4.91[-7] | 4.91[-7] | 4.94[-7] |
| | 4.91[-7],5.99[-10],9.83[-13] | — | — |
| (1,3) | 5.893 637 055 | 5.893 637 055 | 5.893 637 059 |
| | 1.92[-6] | 1.92[-6] | 1.93[-6] |
| | 1.92[-6],3.24[-9],2.69[-13] | — | — |

[a]PED (or ED) with 7/80,[-30,200],[-30,200].
[b]Finite range scattering wave function method with the same basis set and range as present calculation, neglecting background effect [10].
[c]Estimated stable values along $\theta$ trajectory except those in parentheses; see Ref. [24].
[d]Partial widths from high to low asymptotic vibrational state channel. The same for other entries.

this procedure) with small loss in accuracy for low $n_x$ resonance states.

Finally, the present results are compared with those of time delay maximum analysis [10] and complex scaling [24] method in Table IV. The partial widths are also given, which are obtained from the total width and the probability of decaying into each open channel. In particular, they are given by [25]

$$\Gamma_i = F_i \Gamma,$$

where

$$F_i = \frac{|c_i \sqrt{k_i} e^{-ik_i P} f_i(P)|^2}{\sum_j |c_j \sqrt{k_j} e^{-ik_j P} f_j(P)|^2},$$

where $c_i$ is the Siegert eigenvector coefficient of $i$th open channel continuum-type function $f_i$ and $k_i$ is the $i$th channel complex wave number. $P$ is the end point of the integration range. We note excellent agreement between all methods for those resonances reported. (Note that the partial widths shown may not represent the converged values and the earlier complex scaling calculations with a small basis [24] did not report all resonances.)

## IV. CONCLUSIONS

We have shown how the direct Siegert method of finding complex resonance energies and widths corresponding to complex poles of the $S$ matrix can be improved in efficiency. After diagonalization of a single real Hamiltonian matrix we seek the complex Siegert energies by partitioning the eigenproblem to reduce the size of the eigenproblem and combining an individual eigenvalue hunting inverse iteration method with a rational fraction root search method to find each pole. Iterative and complex diagonalizations are completely avoided. This implementation can be used without modification with the infinite range version of the Hamiltonian representation (such as the analytic continuation method of Isaacson, McCurdy, and Miller [3] or the $\hat{H} - E$ combined evaluation method of Yaris, Lovett, and Winkler [4]), provided that the secular determinant equation can be cast into the form of an eigenproblem. However, the finite-range representation used here appears simpler and more efficient for general types of potentials.

It is demonstrated that, in the finite-range version, one can save very substantial computation by using fixed (or almost fixed) continuum-type basis functions to yield a reasonable (or accurate) results when compared with the Siegert-type continuum function case.

The difficulty that arises, that broad resonances are masked by the scattering poles, is inherent in all Siegert methods regardless of the range of the finite basis set used [5]. For this case, if all resonances are desired, a correction scheme or other direct and indirect methods may be used. However, for cases in which only narrow resonances are desired, the present method appears highly advantageous.

## ACKNOWLEDGMENTS

H.W.J. thanks Dr. Seungsuk Han for helpful discussion and for providing rational fraction and root finding subroutines. We acknowledge the support of the National Science Foundation through Grant No. NSF-CHE-9307792.

---

[1] J. N. Bardsley, A. Herzenberg, and F. Mandl, Proc. Phys. Soc. **89**, 305 (1966).
[2] R. A. Bain, J. N. Bardsley, B. R. Junker, and C. V. Sukumar, J. Phys. B **7**, 2189 (1974).
[3] A. D. Isaacson, C. W. McCurdy, and W. H. Miller, Chem. Phys. **34**, 311 (1978).
[4] R. Yaris, R. Lovett, and P. Winkler, Chem. Phys. **43**, 29 (1979).
[5] H.-D. Meyer and O. Walter, J. Phys. B **15**, 3647 (1982).
[6] Y. K. Ho, Phys. Rep. **99**, 1 (1983), for example.
[7] G. Jolicard, C. Leforestier, and E. J. Austin, J. Chem. Phys. **88**, 1026 (1988); U. V. Riss and H.-D. Meyer, J. Phys. B **26**, 4503 (1993).
[8] V. A. Mandelshtam, T. R. Ravuri, and H. S. Taylor, Phys. Rev. Lett. **70**, 1932 (1993); V. A. Mandelshtam, T. R. Ravuri, and H. S. Taylor, Phys. Rev. A **48**, 818 (1993); V. A. Mandelshtam and H. S. Taylor, J. Chem. Phys. **99**, 222 (1993).
[9] F. T. Smith, Phys. Rev. **118**, 349 (1960).
[10] H. W. Jang and J. C. Light, J. Chem. Phys. **99**, 1057 (1993).
[11] A. U. Hazi, Phys. Rev. A **19**, 920 (1979).
[12] D. W. Schwenke and D. G. Truhlar, J. Chem. Phys. **87**, 1095 (1987).
[13] C. Bloch, Nucl. Phys. **4**, 503 (1957); A. M. Lane and D. Robson, Phys. Rev. **151**, 774 (1966); C. W. McCurdy, T. N. Rescigno, and B. I. Schneider, Phys. Rev. A **36**, 2061 (1987).
[14] W. H. Press, B. P. Flannery, S. A. Teukolsky, and W. T. Vetterling, *Numerical Recipes* (Cambridge University Press, Cambridge, MA, 1986).
[15] P. G. Burke and W. D. Robb, in *Advances in Atomic and Molecular Physics,* edited by D. R. Bates and W. D. Robb (Academic Press, New York, 1975), Vol. 11, p. 144.
[16] R. C. Mayrhofer and J. M. Bowman, J. Chem. Phys. **100**, 7229 (1994).
[17] D. Wang and J. M. Bowman, J. Chem. Phys. **100**, 1021 (1994).
[18] A. Maquet, S.-I Chu, and W. Reinhardt, Phys. Rev. A **27**, 2946 (1983).
[19] C. Lanczos, J. Res. Natl. Bur. Stand. **45**, 255 (1950).
[20] D. E. Manolopoulos, M. D'Mello, and R. E. Wyatt, J. Chem. Phys. **91**, 6096 (1989).
[21] J. C. Light, R. M. Whitnell, T. J. Park, and S. E. Choi, in *Supercomputer Algorithms for Reactivity, Dynamics and Kinetics of Small Molecules*, Vol. 227 of *NATO Advanced Study Institute, Series C*, edited by A. Lagana (Reidel Publishing Company, Dordrecht, 1989), p. 187.
[22] E. J. Heller and W. P. Reinhardt, Phys. Rev. A **5**, 757 (1972).
[23] D. E. Manolopoulos and R. E. Wyatt, Chem. Phys. Lett. **152**, 23 (1988).
[24] K. M. Christoffel and J. M. Bowman, J. Chem. Phys. **78**, 3952 (1983).
[25] C. W. McCurdy and T. N. Rescigno, Phys. Rev. A **20**, 2346 (1979).